

Study on Thermal Degradation and Flame Retardant Property of Halogen-Free Polypropylene Composites Using XPS and Cone Calorimeter

Kuang-Chung Tsai,¹ Chen-Feng Kuan,² Chia-Hsun Chen,³ Hsu-Chiang Kuan,² Shu-Wei Hsu,⁴ Fang-Mei Lee,⁵ Chin-Lung Chiang⁴

¹Department of Safety, Health and Environmental Engineering, National Kaohsiung First University of Science and Technology, Kaohsiung, 811, Taiwan

²Department of Computer Application Engineering, Far East University, Tainan 744, Taiwan

³Department of Material Science and Engineering, Far East University, Tainan 744, Taiwan

⁴Department of Safety, Health and Environmental Engineering, Hung Kuang University, Salu, Taichung 433, Taiwan

⁵Department of Child Care and Education, Hung-Kuang University, Salu, Taichung 433, Taiwan

Correspondence to: C.-L. Chiang (E-mail: dragon@sunrise.hk.edu.tw)

ABSTRACT: In this study, the kind of halogen-free flame-retardant containing phosphorus and nitrogen was blended with polypropylene (PP) by hot melt to improve the flame-retardant property of the composites. The cone calorimeter was used to investigate flame-retardant property of the composites. The formation mechanism of the char obtained from the combustion under air atmosphere at 700° was studied by scanning electron microscopy (SEM) and X-ray photoelectron spectroscopy (XPS). Results demonstrated that the PP composite containing nitrogen and phosphorus showed good flame retardancy from cone calorimeter. According to XPS results, it had been found that the intumescent char produces phosphorus and polyphosphorus acid during drastic decomposition, which act as dehydration agents to drive the formation of the heat-resistant carbonaceous char by carbonization. There are also some glass materials, such as P₂O₅ compound, which can benefit the flame retardance. © 2012 Wiley Periodicals, Inc. *J. Appl. Polym. Sci.* 000: 000–000, 2012

KEYWORDS: polypropylene; flame retardant; halogen-free; composite

Received 6 December 2011; accepted 15 March 2012; published online

DOI: 10.1002/app.37700

INTRODUCTION

Polypropylene (PP) is used in many industrial applications because of its low cost and easy processing. These applications require a degree of flame retardancy, which can generally be obtained using additives. Intumescent flame retardants (IFR) for PP have attracted great attention because of its low smoke, low toxicity, no corrosive gas, and no melt dripping during combustion.^{1–5} It is known that a typical IFR system is usually composed of three sources, i.e., an acid source, a carbon source (or char forming agent) and a gas source (or a blowing agent).^{6–11} The mechanism of IFR system is usually described as the following steps^{12–14}: at first, the acid source decomposes to yield a mineral acid, then the acid catalyzes the dehydration process of the charring agent to yield cellular carbonaceous layer, and finally the carbonaceous layer is expanded to form a foam char with nonflammable gas released by blowing agent. The charred layer provides an insulating shield acts as a physical barrier

which limits heat and mass transfer between the gaseous phase and the condensed phase.

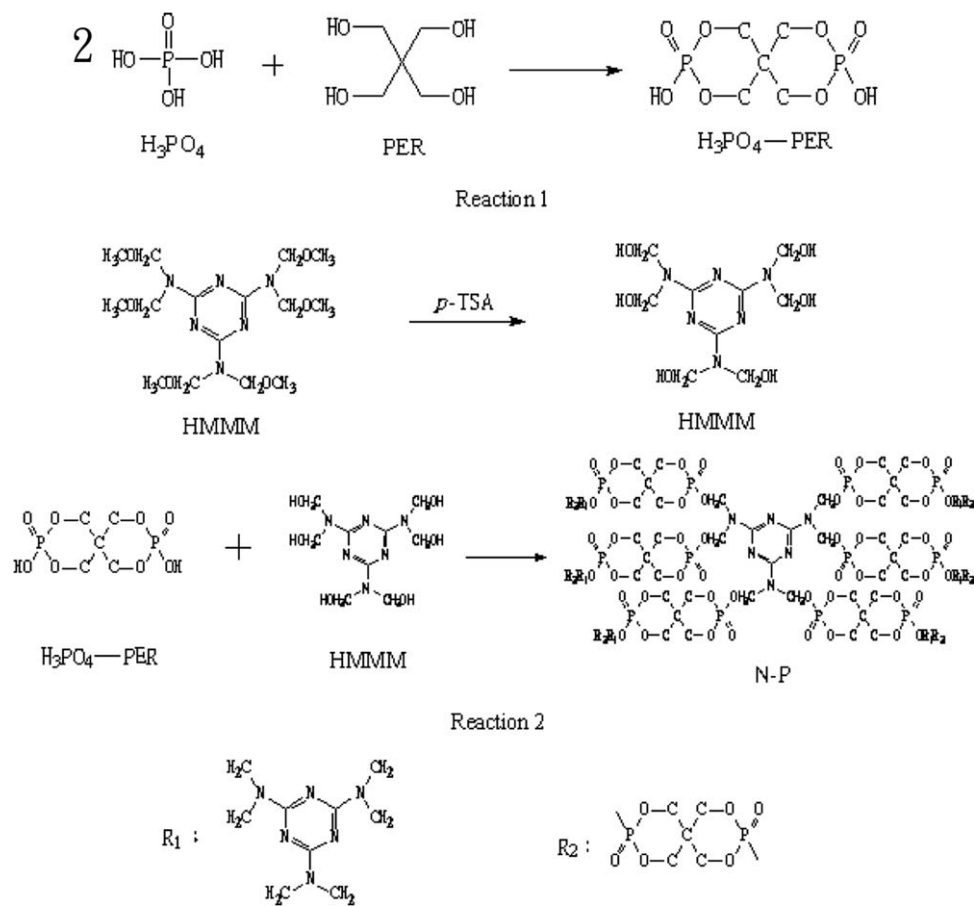
In this study, the kind of halogen-free flame retardant containing phosphorus and nitrogen was blended with PP by hot melt to improve the flame-retardant property of the composites. Phosphorus acid was used as an acid source, pentaerythritol as a carbonization agent and hexamethoxymethylmelamine as a blowing agent. The cone calorimeter was used to investigate flame-retardant property of the composites. The formation mechanism of the char obtained from the combustion under air atmosphere at 700° was studied by scanning electron microscopy (SEM) and X-ray photoelectron spectroscopy (XPS).

EXPERIMENTAL

Materials

Pentaerythritol (PER) was obtained from the Acros Organics, Janssens Pharmaceuticaan, Geel, Belgium. Phosphoric acid

© 2012 Wiley Periodicals, Inc.



Scheme 1. Reaction scheme of the N-P.

(H_3PO_4) was obtained from the Union Chemical Works, Taiwan. Hexamethoxymethylmelamine (HMMM) was supplied by the Cytec Industries, Taiwan. ρ -Toluenesulfonic acid (ρ -TSA) was purchased from the Showa Chemical, Japan. Polypropylene (PP, Yungsox 3005) with M.W. 135,700, m.p. = 180° was supplied as pellets by Formosa Plastics Company, Taiwan.

Preparation of Flame-Retardant Containing Nitrogen and Phosphorus (N-P)

Totally, 8.5 g H_3PO_4 and 5.86 g PER (mole ratio = 2:1) were added into the sample bottle and stirred mechanically at 120° for 4 h to form H_3PO_4 -PER. 5.64 g HMMM and 0.17 g ρ -TSA

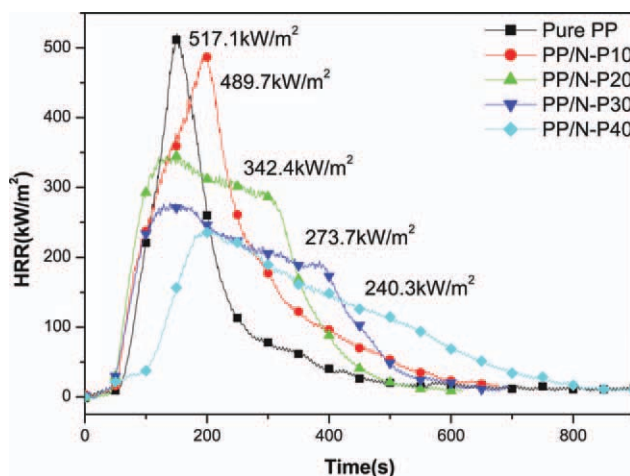


Figure 1. Dynamic curves of HRR data versus time for sample PP/N-P composites. [Color figure can be viewed in the online issue, which is available at wileyonlinelibrary.com.]

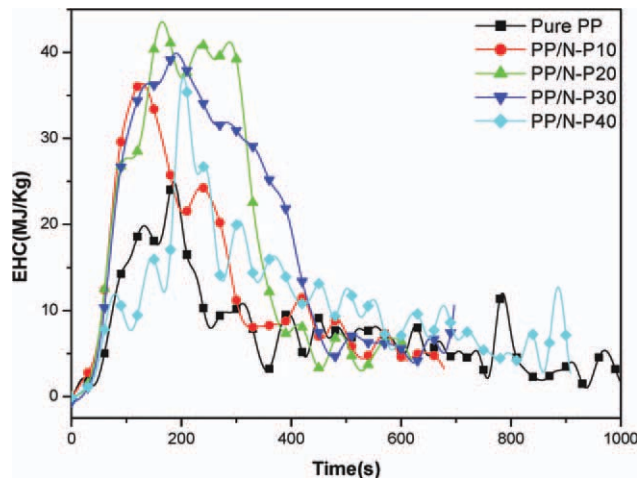


Figure 2. EHC curves versus time for sample PP/N-P composites. [Color figure can be viewed in the online issue, which is available at wileyonlinelibrary.com.]

Table I. Data Recorded in Cone Calorimeter Experiments for PP/N-P Composites

Sample no.	TTI ^a (s)	TFO ^b (s)	PHRR ^c (kW/m ²)	Reduction for PHRR (%)	t _{PHRR} (s)	FGR ^d (kW/m ² s)
Pristine PP	36	423	517.1	-	149	3.5
PP/N-P 10	34	668	489.7	5.3	198	2.5
PP/N-P 20	31	598	342.4	33.8	142	2.4
PP/N-P 30	30	677	273.7	47.1	144	1.9
PP/N-P 40	30	887	240.3	53.5	201	1.2

^a Time to ignition, ^b Time to flameout, ^c Peak heat release rate, ^d Fire growth rate index.

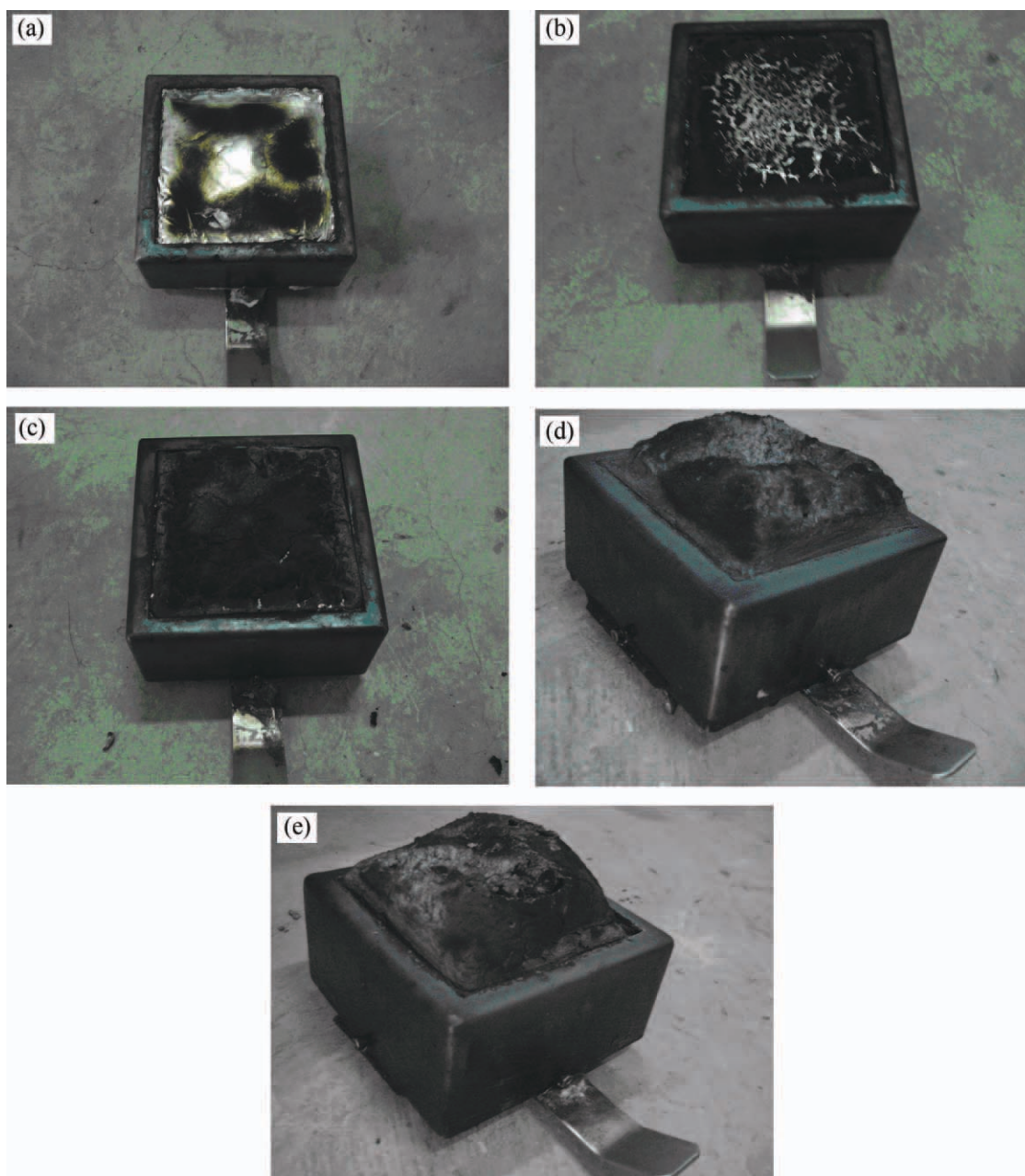


Figure 3. Digital photos of the residue in the cone calorimeter (a) Pristine PP (b) PP/N-P10 (c) PP/N-P 20 (d) PP/N-P 30 (e) PP/N-P 40. [Color figure can be viewed in the online issue, which is available at wileyonlinelibrary.com.]

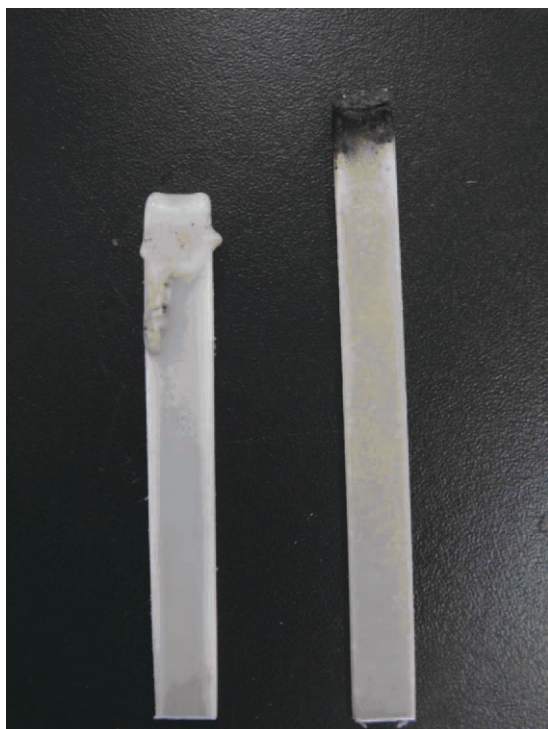


Figure 4. Digital photos of residues after burning for 30 s (a) Pristine PP and (b) PP/N-P30 composites. [Color figure can be viewed in the online issue, which is available at wileyonlinelibrary.com.]

were poured into H_3PO_4 -PER at 120° for 3 h to produce flame-retardant containing nitrogen and phosphorus, N-P.

Preparation of PP/N-P Composites

All samples were mixed as 50 g batches of PP with the desired amounts of N-P for 8 min at 180°C using Brabender mixer (Type: Plastograph[®] EC Plus, Brabender[®] GmbH, Germany). The resulting mixtures were then compression molded at 185°C into sheets (3 mm thickness) under a pressure of 9 MPa for 10 min. The sheets were cut into suitable size specimens for fire testing.

Reaction Schemes

The novel composites were prepared as described in Scheme 1.

Cone Calorimeter

A cone calorimeter (Stanton Redcroft type, made in England) was used to measure the flammability characteristics with $100 \times 100 \times 3$ specimens. Each specimen was wrapped in an aluminum foil and exposed horizontally to 35 kW/m^2 external heat flux.

X-Ray Photoelectron Spectra

XPS were recorded using a PHI Quantera SXM/Auger, with Al K α excitation radiation ($h\nu = 1486.6 \text{ eV}$). The pressure in the analyzer was maintained at about $6.7 \times 10^{-7} \text{ Pa}$. XPS data were processed by DS 300 data system.

Scanning electron microscope

The morphology of the fractured surface of the composites was examined using a SEM (JEOL JSM 840A, Japan).

RESULTS AND DISCUSSION

Flame-Retardant Property of Composites

Cone calorimetry is used to evaluate the flammability and potential fire safety of polymer materials under well-ventilated conditions, which remains one of the most effective bench-scale tests that is used to predict the combustion behaviors of materials in a real fire.^{15,16} The material burns under homogeneous forced flaming conditions in the cone calorimeter. The heat release rates (HRRs) vs. time curves for pristine PP and PP/N-P composites are presented in Figure 1 and the results are listed in Table I. It is noteworthy that pure PP burns very rapidly after ignition and the peak heat release rate (PHRR) is 517.1 kW/m^2 . The values of PHRR of composites decrease with the increasing of N-P contents. As expected, PP/N-P composites which contain 40 wt % N-P exhibits a considerable reduction in HRR and PHRR decreases to 273.7 kW/m^2 , decreasing by 47%. It may be due to the fact that PP/N-P forms a stable and compact char layer, which retards the transfer of heat inside the specimen during the ignition process, thus improving the flame properties. It can be seen in Figure 1 that the HRR curve of PP/N-P is flatter than that of pristine PP and the values of HRR of composites

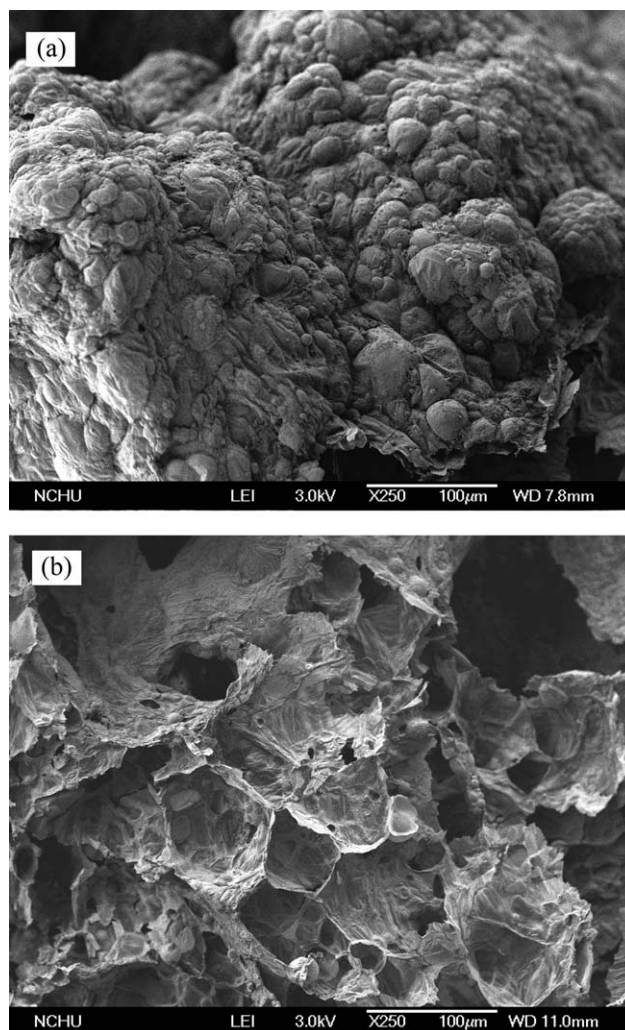


Figure 5. SEM of intumescent char for PP/N-P 30 composite (a) outer surface (b) inner surface ($\times 250$).

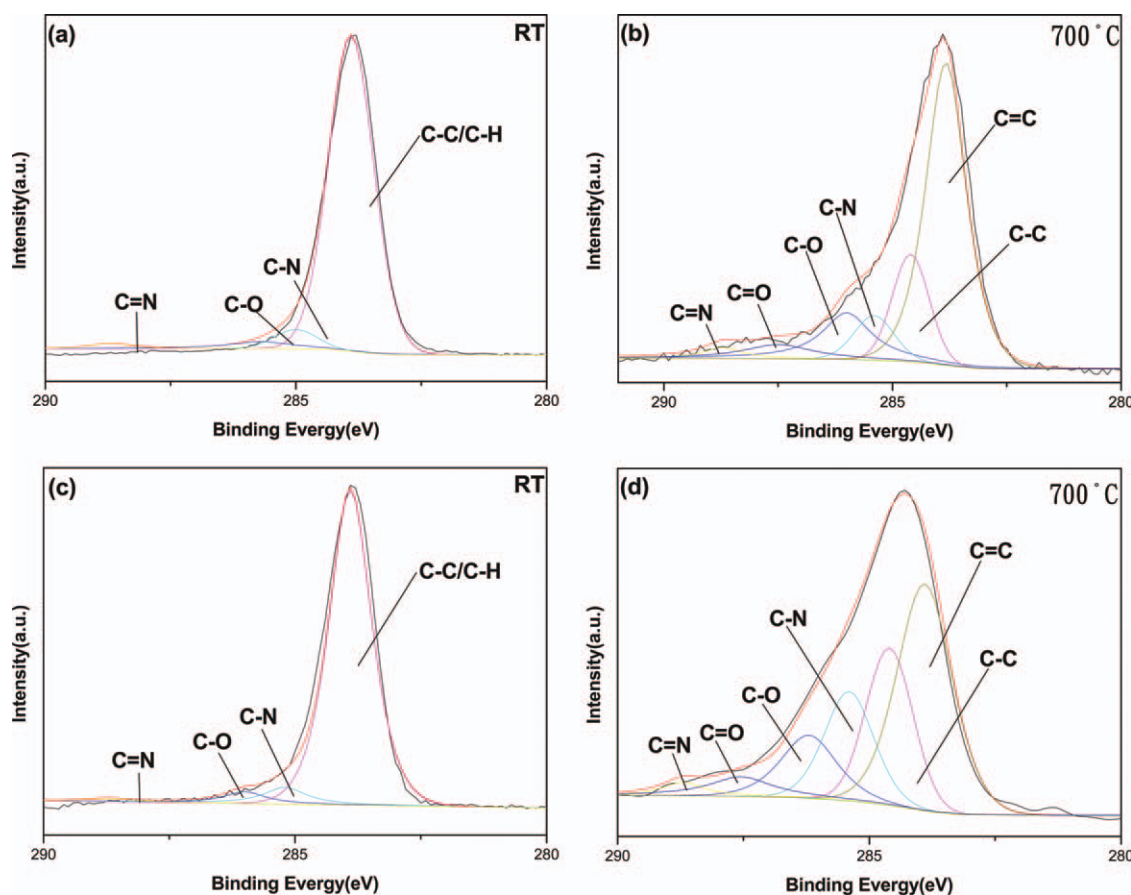
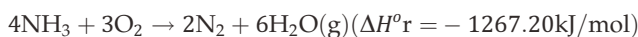


Figure 6. C1s spectra of composite under air atmosphere (a) PP/N-P10 at room temperature (b) PP/N-P10 at 700° for 30 min. (c) PP/N-P30 at room temperature (d) PP/N-P30 at 700° for 30 min. [Color figure can be viewed in the online issue, which is available at wileyonlinelibrary.com.]

decrease sharply compared with that of PP. The HRR curve of the PP/N-P is typical of IFR systems. The HRR curve exhibits shoulder shape. The earlier shoulder is assigned to the ignition and to the formation of an expanded protective shield during lower temperature range; the later shoulder is explained by the destruction of the intumescent structure and the formation of a carbonaceous residue during higher temperature range.¹⁷

Figure 2 shows the effective heat of combustion (EHC) values of the test samples. The EHC data is estimated by the ratio of heat to mass loss. EHC indicates the efficiency of combustion of the volatiles produced from thermal degradation of materials, which can be used to understand mechanism of fire degradation of materials. According to Figure 2, the values of EHC for the composites are little higher than that of pure polypropylene. The higher EHC indicates that the volatiles produced are easier to burn in the gas phase. The materials containing HMMM will produce solid chars of melam and melam and release NH₃ into gas phase. Ammonia gas was burned on heating and gave off heat. The combustion heat of ammonia gas which is calculated according the following equation resulted in higher EHC values.



Time to ignition (TTI) is used to determine the influence on ignitability, which can be measured from the onset of an HRR

curve. As shown in Figure 1 and listed in Table I, the TTI of pristine PP is 36 s, while that of PP/N-P40 decreases to 30 s, decreasing by 17%. The reason for this may be due to the fact that the N-P decomposes at relatively low temperature, releasing small volatile molecules, which causes the samples to burn more easily under the radiation of thermal flux.

The Fire Growth Rate Index (FGRI) is calculated by dividing PHRR by t_{PHRR} , giving a unit of kW/m² s, which can estimate both the predicted fire spread rate and the size of a fire. The higher the FGRI, the faster the flame spread and flame growth is assumed to be.^{18,19} From Table I, the values of FGRI for composites decrease with the increasing of N-P contents. The FGRI of pristine PP is 3.5 kW/m² s, while that of PP/N-P40 decreases to 1.2 kW/m² s, decreasing by 66%. It means that N-P performs good flame-retardant behaviors.

The appearance of PP/N-P composite residues at the end of cone calorimeter tests is shown in Figure 2. It is clear that there is almost no residue left at the end of the cone calorimeter test for pristine PP composite from Figure 2(a). It means that PP is highly flammable. It can be seen that sparse char left due to insufficient flame retardant in Figure 2(b,c). On the other hand, the surface of the PP/N-P residue is covered with an expanded thick and solid char network in Figure 2(d,e). The residue left

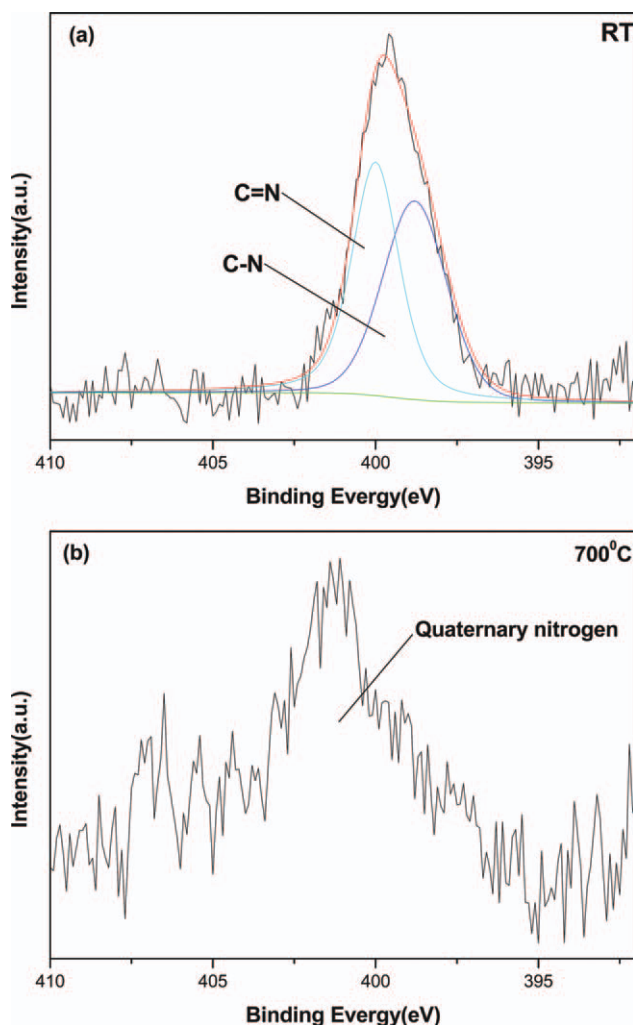


Figure 7. N1s spectra of PP/N-P30 (a) room temperature (b) under air atmosphere at 700° for 30 min. [Color figure can be viewed in the online issue, which is available at wileyonlinelibrary.com.]

by PP/N-P is mainly formed of thick expanded black char, and the char is better than that of PP in protecting the underlying materials. The results indicate that a good and coherent char can prevent the heat transfer and flame spread, and thus protect the underlying materials from further burning.

Morphological Property of Composites

Figure 3(a,b) showed digital photos of residues after burning for 30 s for pristine PP and PP/N-P30 composite, respectively.

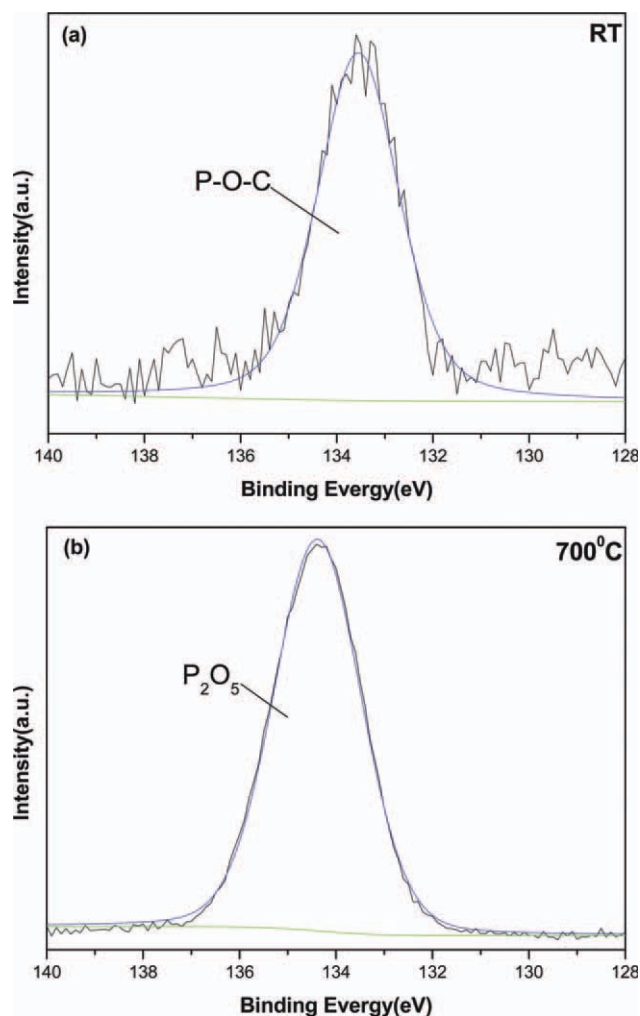


Figure 8. P2p spectra of PP/N-P30 (a) room temperature (b) under air atmosphere at 700° for 30 min. [Color figure can be viewed in the online issue, which is available at wileyonlinelibrary.com.]

It was found out that pristine PP performs obvious appearance of dripping owing to thermoplastic from Figure 3(a). It will spread out fire after it was melted under high temperature range. According to Figure 3(b), PP/N-P 30 did not take place the dripping phenomena. When the sample was ignited, the fire on the sample was extinguished rapidly after the Bunsen burner was moved away. It means the char can stop the fire growth.

Figure 4 showed SEM of intumescent char for PP/N-P 30 composite (a) outer surface (b) inner surface. From Figure 4(a), the

Table II. Binding Energy (eV) and Relative Peak Intensities (%) of the Various Components of C1s Peak-Fitted Signals

Sample no.	C1s (%)					
	C-N 285.4 eV	C=N 288.7 eV	C-C/C-H 284.6 eV	C=C 283.9 eV	C-O 286.3 eV	C=O 287.6 eV
PP/N-P10 at RT	5	1	90	-	4	-
PP/N-P10 at 700°	7	3	16	54	14	6
PP/N-P30 at RT	6	1	88	-	5	-
PP/N-P30 at 700°	17	3	23	40	12	5

Table III. The Values of C_{ox}/C_a of Composites at Room Temperature and 700°

Sample no.	Temperature	
	Room temperature	700°
PP/N-P10	0.04	0.25
PP/N-P30	0.05	0.20

structure of the charring layer inclines to be more compact and more homogeneous, the intension of charring layer improves largely, and the effect of the flame retardant is better. There are many irregular mini-pore structures of spongy foams in the charring layer from Figure 4(b). It explains the dehydration charring of PER and frothing of HMMM proceeds in the range of rather appropriate temperature. Moreover, the intumescent layer is compact and spongy, and the heat insulation effect. The different aperture surface tensions in the course of gas cavities lead to the asymmetry of abscess, and the surface tension relies on the viscosity and symmetry of the coating. The intumescent charring layer with many mini-pores acts as the effect of the flame retardant, heat insulation, and protecting inner matrix materials.

XPS for Char Analysis

As for the intumescent flame-retardant system, it is noted that the intumescent char influences the flame retardancy and thermal degradation of the composites greatly.²⁰ In this work, we hypothesized that the thermal stability of the intumescent coatings were influenced by the contents of N-P, so the residue chars of the intumescent coatings with different contents of additives were prepared at room temperature (RT) and 700° in the muffle furnace for 10 min under air atmosphere and then analyzed by XPS spectroscopy. The aim of the XPS analysis was to study the influence of contents N-P on the carbonization and degradation process and the role of flame retardant from Figures 5–8 and Tables II and III.

The C1s spectra are shown in Figure 5 and Table II summarizes the results of the most probable fit assumptions. For the samples at room temperature, four peaks were distinguished. The bands around 285.4, 288.7, 284.6, and 286.3 eV may be assigned to C–N, C=N, C–C/C–H, and C–O, respectively.^{21–23} For the samples heated at 700° under air atmosphere, additional two peaks were found out. The bands around 283.9 eV and 287.6 eV may be assigned to C=C and C=O, respectively. From Table II, the C–C groups may be transformed into species containing C=C as indicated by the existence of the band centered at about 283.9 eV in C1s spectra during the heating course. It means that aliphatic carbons were changed into graphitic carbons, which indicated the formation of char.

To the thermal stability of the residue chars, the ratio of oxidized carbons to nonoxidized carbons can indicate the thermal stability of char layer. The values of the ratio of C_{ox} (oxidized carbons) to C_a (aliphatic, aromatic carbons, and other nonoxidized carbons) are given in Table III. At 700°, C_{ox}/C_a was 0.25 (PP/N-P 10) and 0.20 (PP/N-P 30), respectively, which indicated N-P deferred the degradation of the intumescent chars at this temperature. The evidence shows that more N-P flame retardant can promote the thermal stability of the residue chars.

Figure 6(a,b) present N1s spectra of PP/N-P30 at room temperature and under air atmosphere at 700° for 30 min, respectively. In Figure 6(a), the N1s peaks at 398.3 and 400.0 eV can be attributed to C–N and C=N, respectively. From Figure 6(b), the shoulder peak appears at 401.2 eV, which could be a result of the formation of quaternary nitrogen and to formation of some oxidized nitrogen compounds, as reported in the literature.²⁴ It was found out that the intensity of the peak at around 401.2 eV is less than those of C–N and C=N. It means that melamine groups of HMMM decompose at temperatures above 350°C releasing of considerable quantize of ammonia gas to expand formed char and forming highly thermal stable intumescent melam and melem products which can prevent further thermal degradation.^{25–28}

Figure 7(a,b) present P2p spectra of PP/N-P30 under air atmosphere at room temperature and at 700° for 30 min, respectively. Binding energies of 133.5 eV have been assigned to P–O–C groups²⁷ in Figure 7(a). From Figure 7(b), the band around 134.4 eV can be assigned to P=O group in phosphate species

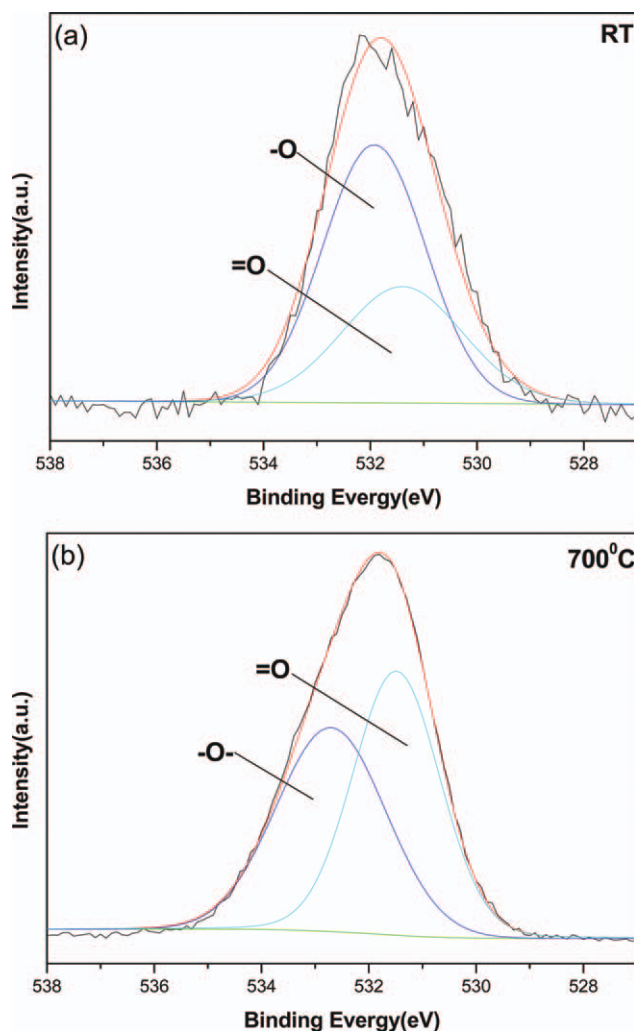


Figure 9. O1s spectra of PP/N-P30 of (a) at room temperature (b) the heat-treated for 30 min under air atmosphere at 700°. [Color figure can be viewed in the online issue, which is available at wileyonlinelibrary.com.]

(e.g., P=O phosphoric acid or polyphosphoric acid) or inorganic phosphorus-containing species (e.g., P₂O₅),²⁸ which form during the thermal degradation of phosphorus-containing compounds.²⁹

The O1s spectra are shown in Figure 8. According to the literature, it is impossible to distinguish the inorganic oxygen from the organic oxygen because the O1s band is structureless.³⁰ The peaks around 531.4 eV can be assigned to the =O in phosphate or carbonyl groups and the peak in the vicinity of 532.2 eV is caused by —O— in P—O—P, C—O—P, and/or C—OH groups.^{31–35} Compared Figure 9(a,b), it can be found out that the area of the =O is increasing and the area of —O— is decreasing simultaneously. It means the oxidation reaction takes place at high temperature.

The evidences show that N-P produces phosphorus and polyphosphorus acid during drastic decomposition, which act as dehydration agents to drive the formation of the heat-resistant carbonaceous char by carbonization. There are also some glass materials, such as P₂O₅ compound, which can benefit the flame retardance.

CONCLUSIONS

In this study, cone calorimeter testing demonstrates that the incorporation of nitrogen and phosphorus into PP could improve the flame retardancy of the material effectively. The values of PHRR and FGRI of composites decrease with the increasing of N-P contents, which indicated the additives benefit the flame retardance. SEM results show that the intumescent charring layer with many mini-pores acts as the effect of the flame retardant, heat insulation, and protecting inner matrix materials. XPS spectra of C, O, N, and P show that aliphatic carbons were changed into graphitic carbons, which indicated the formation of char. Highly thermal stable intumescent melam and melem products was formed and prevent further thermal degradation. Phosphorus components produce inorganic glass compound which can stop flame spread. During the combustion process of the PP/N-P composite, the formation of a stable intumescent char could protect the underlying materials from the heat and flame and thus enhance the flame retardancy of the material.

ACKNOWLEDGMENTS

Contract grant sponsor: National Science Council of the Republic of China; contract grant number: NSC-100-2628-E-241-002.

REFERENCES

- Du, B.; Guo, Z.; Fang, Z. *Polym. Degrad. Stab.* **2009**, *94*, 1979.
- Li, B.; Xu, M. *Polym. Degrad. Stab.* **2006**, *91*, 1380.
- Peng, H. Q.; Zhou, Q.; Wang, D. Y.; Chen L.; Wang, Y. Z. *J. Ind. Eng. Chem.* **2008**, *14*, 589.
- Chiu, S. H.; Wang, K. W. *Polymer* **1998**, *39*, 1951.
- Chou, C. S.; Lin, S. H.; Wang, C. I. *Adv. Powder Technol.* **2009**, *20*, 169.
- Hendrickson, L.; Connoles, K. B. *Polym. Eng. Sci.* **1995**, *35*, 211.
- Riva, A.; Camino, G.; Fomperie, L.; Amiquet, P. *Polym. Degrad. Stab.* **2003**, *82*, 341.
- Bourbigot, S.; Le Bras, M. *Carbon* **1995**, *33*, 283.
- Le Bras, M.; Bourbigot, S.; Christelle, D. *Fire Mater* **1996**, *20*, 191.
- Almeras, X.; Le Bras, M.; Hornsby, P.; Bourbigot, S. *Polym. Degrad. Stab.* **2003**, *82*, 325.
- Almeras, X.; Dabrowski, F.; Le Bras, M.; Delobel, R.; Bourbigot, S.; Marosi, G.; Anna P. *Polym. Degrad. Stab.* **2002**, *77*, 305.
- Camino, G.; Costa, L.; Martinasso, G. *Polym. Degrad. Stab.* **1989**, *23*, 359.
- Xie, F.; Wang, Y. Z.; Yang, B.; Liu, Y. *Macromol. Mater. Eng.* **2006**, *291*, 247.
- Samyn, F.; Bourbigot, S.; Duquesne, S.; Delobel, R. *Thermochim. Acta* **2007**, *456*, 134.
- Babrauskas, V. *Fire Mater.* **1995**, *19*, 243.
- Babrauskas, V.; Peacock, R. D. *Fire Safety J.* **1992**, *18*, 255.
- Bourbigot, S.; Le Bras, M.; Duquesne, S.; Rochery, M. *Macromol. Mater. Eng.* **2004**, *289*, 499.
- Messerschmidt, B.; Hees, P. V. *Fire Mater.* **2000**, *24*, 121.
- Nazare, S.; Kandola, B.; Richard, H. A. *Fire Mater.* **2002**, *26*, 191.
- Camino, G.; Costa, L.; Luda di Cortemiglia, M. P. *Polym. Degrad. Stab.* **1991**, *33*, 131.
- Chen, X.; Hu Y.; Jiao, S. L. *Polym. Degrad. Stab.* **2007**, *92*, 1141.
- Peng, H. Q.; Wang, D. Y.; Zhou, Q.; Wang, Y. Z. *Chin. J. Polym. Sci.* **2008**, *26*, 299.
- Zhou, S.; Song, L.; Wang, Z.; Hu, Y.; Xing, W. *Polym. Degrad. Stab.* **2008**, *93*, 1799.
- Beamson, G.B. D. *High Resolution XPS of Organic Polymers*; Chichester: Wiley; **1992**.
- Shieh, J. Y.; Wang, C. S. *Polymer* **2001**, *42*, 7617.
- Wang, C. S.; Lin, C. H. *J. Polym. Sci. Polym. Chem.* **1999**, *37*, 3903.
- Onoa, S.; Funato, T.; Inoue, Y.; Munechika, T.; Yoshimura, T.; Morita, H.; Rengakuji, S. I.; Shimasaki, C. J. *Chromatogr. A* **1998**, *815*, 197.
- Lotsch, B. V.; Schnick, W. *Chem. Eur. J.* **2007**, *13*, 4956.
- Bourbigot, S.; Lebras, M.; Delobel, R. *Carbon* **1993**, *31*, 1219.
- Clark, D. T.; Fok, T.; Roberts, G. G.; Sykes, R. W. *Thin Solid Films* **1980**, *70*, 261.
- Delpeux, S.; Beguin, F.; Benoit, R.; Erre, R.; Manolova, N.; Rashkov, I. *Eur. Polym. J.* **1998**, *34*, 905.
- Brown, N.M. D.; Hewitt, J. A.; Meenan, B. J. *Surf. Interface Anal.* **1992**, *18*, 187.
- Shih, P. Y.; Yung, S. W.; Chin, T. S. *J. Non-Cryst. Solids* **1998**, *224*, 143.
- Jansen, R.J. J.; Vanekum, H. V. *Carbon* **1995**, *33*, 1021.
- Gonzalez-Elipse, A. R.; Martinez-Alonso, A.; Tascon, J. M. D. *Surf. Interface Anal.* **1988**, *12*, 565.